

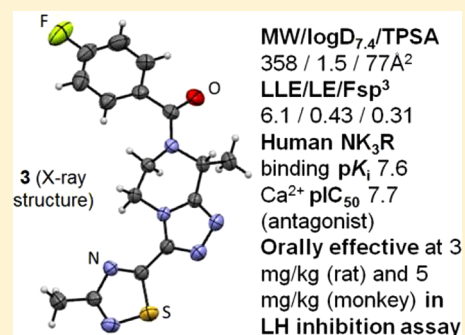
Optimization of Novel Antagonists to the Neurokinin-3 Receptor for the Treatment of Sex-Hormone Disorders (Part II)

Hamid R. Hoveyda,* Graeme L. Fraser, Guillaume Dutheil, Mohamed El Bousmaqui, Julien Korac, François Lenoir, Alexey Lapin, and Sophie Noël

Euroscreen SA, 47 rue Adrienne Bolland, 6041 Gosselies, Belgium

Supporting Information

ABSTRACT: Further lead optimization on *N*-acyl-triazolopiperazine antagonists to the neurokinin-3 receptor (NK₃R) based on the concurrent improvement in bioactivity and ligand lipophilic efficiency (LLE) is reported. Overall, compound 3 (LLE > 6) emerged as the most efficacious in castrated rat and monkey to lower plasma LH, and it displayed the best off-target safety profile that led to its clinical candidate nomination for the treatment of sex-hormone disorders.



KEYWORDS: NK₃ antagonist, triazolopiperazine, neurokinin B, LH, FSH, GnRH

The neurokinin-3 receptor (NK₃R) is a class A GPCR with neurokinin B (NKB) as its endogenous agonist. We present here the sequel on the lead optimization of *N*-acyl-triazolopiperazine NK₃R antagonists (1 and 2, Figure 1).¹

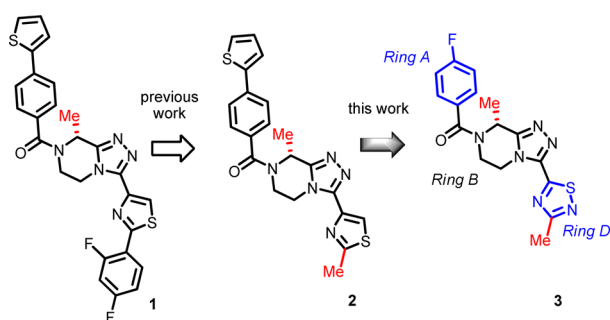


Figure 1. Lead progression: iv POC (1), oral POC (2), and clinical candidate (3). (The “magic methyl” groups are shown in red.)

NK₃R antagonists were speculated as therapeutically relevant for CNS dysfunctions, e.g., schizophrenia, predicated on the “hyperdopaminergic hypothesis”, which repeatedly met with clinical failures in over a decade of efforts.² Meanwhile, emerging biology has unambiguously established the role of NK₃R/NKB signaling in reproductive neuroendocrinology. Importantly, recent studies have revealed NK₃R as a key regulatory component of the hypothalamic–pituitary–gonadal (HPG) axis wherein its tonic activation positively regulates the gonadotropin-releasing hormone (GnRH) pulse frequency.³ In turn, the GnRH pulse frequency is known to differentially control the circulating levels of luteinizing hormone (LH)

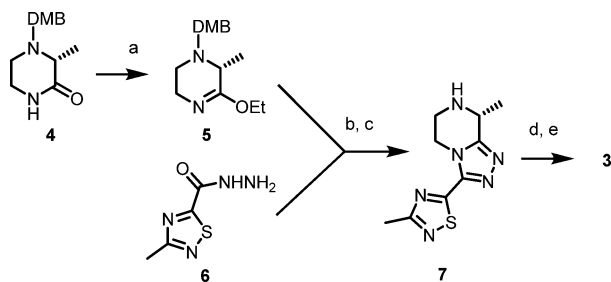
versus follicle-stimulating hormone (FSH). Thus, high frequency pulses stimulate LH release, whereas low frequency pulses favor FSH induction.⁴ These gonadotropins ultimately act on the ovary and testis to promote production of gametes and sex-hormone release. In 2011, it was reported that patients with a loss of function mutation in NK₃R display a phenotype of normosomic congenital hypogonadotropic hypogonadism, low plasma LH, and attendant low LH/FSH ratios that could be restored through exogenous administration of GnRH.⁵ We have demonstrated elsewhere⁶ that the foregoing NK₃R antagonists slow the LH pulse and decrease circulating LH levels without affecting FSH, consistent with the literature reports.⁴ As such, these antagonists are subtle modulators of gonadotropin secretion unlike GnRH ligands that abrogate both LH and FSH with the consequent decline in plasma estrogen to castration levels thereby triggering menopausal-like adverse events such as bone mineral density loss and incidences of hot flashes.⁷ Hence, NK₃R antagonists offer a potentially safer therapeutic approach due to a decreased rather than abrogated GnRH pulse frequency. Collectively, these findings offer a strong rationale for repositioning NK₃R antagonists to address sex-hormone disorders such as polycystic ovary syndrome (PCOS) and uterine fibroids (UF), among others.⁸

The synthetic approach to the analogues herein was previously described.¹ With minor modifications, Scheme 1 was used for the GMP scale-up of 3 in overall 42% yield (2.7 kg) with 99.3% purity and >99.9% enantiomeric excess.

Received: March 17, 2015

Accepted: May 19, 2015

Published: May 19, 2015

Scheme 1^a

^aReagents and conditions: (a) Et_3OBF_4 , Na_2CO_3 , CH_2Cl_2 , 45 min, 68%; (b) MeOH , 70°C , 8 h, 80%; (c) TFA , 2 h, >99% conversion; (d) 4-fluorobenzoyl chloride, NaHCO_3 , 15 min, 97%; (e) recrystallization ($\text{EtOH}/\text{H}_2\text{O}$), 97% (DMB = 2,4-dimethoxybenzyl).

The *in vitro* bioactivity structure–activity relationship (SAR) was established through radioligand binding (pK_i) and aequorin functional assays (pIC_{50}) data from recombinant human NK_3R in CHO cells. The lead optimization strategy¹ of combined improvement in both bioactivity and ligand lipophilic efficiency ($\text{LLE} = \text{pK}_i - \log D_{7.4}$)⁹ was maintained. An initial emphasis was placed on LLE as a predictive marker of improved safety profiles.¹⁰ Other efficiency metrics such as LE^{11} and Fsp^{12} (Table 1) were also tracked, though not as a primary focus. The previously discovered “magic methyl” groups in Rings B and D (Figure 1),¹ so-called due to their significant impact in improving potency and LLE, remained crucial and rendered feasible improvements in Fsp^3 and LE as well (see below).

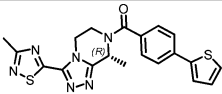
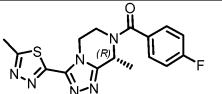
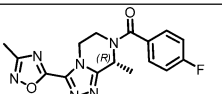
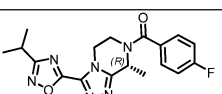
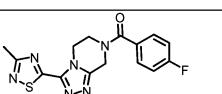
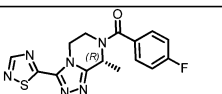
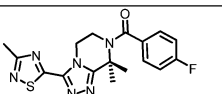
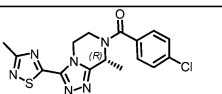
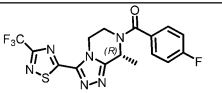
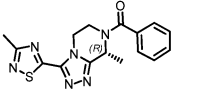
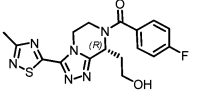
To recall, replacing 2-methylthiazole (2) at Ring D with 3-methyl-1,2,4-thiadiazole (8) was reported earlier to markedly improve bioactivity and LLE (Table 1).¹ Moreover, 1,2,4-thiadiazole is regarded as a means of circumventing bioactivation liabilities potentially relevant to the thiazole ring.¹³ These considerations overall prompted us to retain the 1,2,4-thiadiazole, but to modify the 4-(thiophen-2-yl)phenyl in 8 to the 4-fluorophenyl Ring A (i.e., 3) present in the earlier lead structures.¹ Progression from 8 to 3 helped reduce lipophilicity ($\Delta\log D_{7.4} = -1.5$), which not surprisingly right-shifted bioactivity by nearly one log. However, in evaluating 3 against 8, the improved LLE and absence of the thiophene ring (a potential structural safety alert)¹⁴ was considered of greater importance due to the reduced toxicological risk. In addition, 3 was nearly equipotent to the oral POC lead 2, while >1-log superior in LLE. Narrowing our focus on the thiadiazole Ring D and related variants, we observed the following descending trend in bioactivity (Table 1): 1,2,4-thiadiazole (3) > 1,2,4-oxadiazole (10) \gg 1,3,4-thiadiazole (9). As with the Ring A cases, increased lipophilicity in Ring D helped improve bioactivity albeit offset by a loss in LLE, e.g., 11 vs 10 (Table 1). The impact of Rings B and D magic methyl groups on SAR trends was quite pronounced, as expected based on previous results,¹ since the corresponding *des*-Me analogues of 3, whether at Ring B or D (12 and 13, respectively), were decidedly inferior in both bioactivity and LLE (Table 1). *Gem* dimethyl Ring B substitution substantially eroded the bioactivity (14 vs 3) in keeping with the unfavorable impact of (*S*)-Me at this Ring B position (data not shown).¹ Once again, improved bioactivity followed increased lipophilicity whether at Ring A (15) or at Ring D (16) positions, but this gain was negated by a deteriorated LLE against 3. Conversely, replacing 4-fluorophenyl with phenyl at Ring A, i.e., 17, helped diminish lipophilicity, but it also deteriorated bioactivity.

Interestingly, a hydroxyethyl substitution at Ring B (18) afforded an alternative means of reducing lipophilicity ($\Delta\log D_{7.4} = -0.5$ vs 3) with minimal impact on bioactivity, thus resulting in a 0.4-log superior LLE vs 3. Despite this, 18 proved inferior to 3 due to P_{gp} efflux that in turn markedly diminished its brain exposure level (Table 2 and discussion further below).

The hERG SAR herein (Table 1) was governed by the interplay between lipophilicity and the hydrogen-bond acceptor (HBA) count in the heteroaryl Ring D, as previously reported.¹ For instance, in progressing from 8 to 3 ($\Delta\log D_{7.4} = 1.5$), the hERG IC_{50} was improved by over 12-fold. However, the poor hERG $\text{IC}_{50} = 1.6\ \mu\text{M}$ in 11 ($\log D_{7.4} = 1.7$) was in keeping with the increased HBA count in the Ring D oxadiazole (N + N + O) in stark contrast to the thiadiazole (N + N) Ring D variations (3 and 15–18), all of which displayed a superior hERG, $\text{IC}_{50} \geq 39\ \mu\text{M}$ ($\log D_{7.4} = 1.3$ – 2.4). Interestingly, the Ring B hydroxyl group in 18 did not adversely impact hERG ($\text{IC}_{50} = 50\ \mu\text{M}$) suggesting that the HBA effect on hERG SAR is primarily a Ring D related effect. Finally, the Ring B magic methyl also reduced hERG efficacy, i.e., 3 ($\text{IC}_{50} > 100\ \mu\text{M}$) vs 12 ($\text{IC}_{50} = 50\ \mu\text{M}$). Compound 3 was the best overall in the hERG and CYP safety profile evaluation.

Based on the free drug hypothesis, the unbound fraction rather than total drug is relevant for PKPD analysis.¹⁵ The NK_3R is mainly expressed on KNDy neurons in the ARC region of the hypothalamus³ that is part of the circumventricular organs lacking blood–brain barrier and are therefore exposed to blood solutes.¹⁶ As such, both the unbound plasma (f_u) and the unbound brain levels (bf_u) must be considered here (Table 2). While lipophilicity alone does not correlate well to albumin binding, this trend is often apparent in a congeneric series.¹⁷ Hence, a compound with balanced lipophilicity such as 3 ($\log D_{7.4} = 1.5$) displayed high f_u and bf_u levels (>50%) in contrast to the more lipophilic congeners, e.g., 16 (Table 2). It is noteworthy that despite an increase in unbound plasma concentration, the systemic clearance levels (CL_T) remained low (e.g., 3, Table 2). The comparatively lower CL_T in para substituted phenyl Ring A (3, 15) against the unsubstituted congener 17 is likely due to the metabolic blocking effect. All analogues except 18 displayed high Caco-2 permeability with no evidence of appreciable P_{gp} efflux ($\text{ER} = 0.6$ – 1.2), consistent with the high oral availability (%F) and brain-to-plasma ratios observed. The so-called P_{gp} rule-of-4 suggests that increasing the number of HBA atoms to (N + O) ≥ 8 tends to confer an increasing likelihood of P_{gp} efflux.¹⁸ This is in keeping with the P_{gp} efflux in 18 ($\text{ER} = 3.8$) given its HBA atom count (N + O = 8). As with 2,¹ a complete oral absorption (%F > 100) was also observed in rat with compound 12 and in monkey with 3. This phenomenon is well-known and various underlying causes have been reported.¹⁹ No drug accumulation was observed in 5-day once-daily oral dosing studies in rats (3 and 12) or monkeys (3), despite administration of elevated doses (e.g., up to 1 g/kg in rats with 12), in step with the relatively short half-life values and the previous related observations with 2.¹ Moreover, no adverse hepatotoxicity (AST, ALT, and bilirubin levels normal) was detected in these subchronic studies. Furthermore, 3 displayed the highest $\text{bf}_u = 0.525$ and brain unbound concentration ($\text{C}_{\text{brain,u}} = 343\ \text{nM}$) herein (Table 2). In contrast, 18 although nearly completely unbound in the brain displayed a comparatively low $\text{C}_{\text{brain,u}} = 45.6\ \text{nM}$ consistent with its elevated P_{gp} efflux ratio.

Table 1. Human NK₃R In Vitro Bioactivity, LogD_{7.4}, Ligand Efficiency Metrics,^{10–12} and Off-Target Safety SAR

Cpd	Structure	pK _i , pIC ₅₀	logD _{7.4} ^a	LLE	LE	Fsp ³	CYP panel IC ₅₀ (μM) ^b	hERG (μM) ^c	IC ₅₀
1	See Figure 1	8.7, 7.7	5.0	3.7	0.33	0.15	19, 7, 3, 4, 21	1.4	
2	See Figure 1	7.9, 7.8	3.1	4.8	0.38	0.24	50, >100, 21, 34, 26	24	
3	See Figure 1	7.6, 7.7	1.5	6.1	0.43	0.31	90, >100, 42, 48, >100	>100	
8		8.5, 8.4	3.0	5.5	0.41	0.24	79, 39, 13, 19, 67	8	
9		5.0, 4.8	0.8	4.2	0.28	0.31	--	--	
10		6.9, 6.8	0.7	6.2	0.39	0.31	>100, >100, 42, 34, 86	--	
11		7.6, 7.4	1.7	5.9	0.39	0.39	>100, >100, 64, 56, 100	1.6	
12		7.0, 6.8	1.2	5.8	0.41	0.27	>100, >100, 82, 56, >100	50	
13		5.9, 5.9	1.1	4.8	0.34	0.27	--	--	
14		6.7, 6.2	2.0	4.7	0.36	0.35	>100, >100, 12, 4, 51	--	
15		7.7, 7.5	2.0	5.7	0.43	0.31	>100, 88, 7, 50, 99	66	
16		8.1, 8.2	2.4	5.7	0.40	0.31	>100, >100, 45, 57, 54	39	
17		7.3, 7.2	1.3	6.0	0.42	0.31	31, >100, 12, 17, 63	50	
18		7.5, 7.1	1.0	6.5	0.39	0.35	>100, >100, 77, 54, >100	50	

^aN = 3, %RSD ≤ 5. ^bCYP 3A4, 2D6, 2C9, 2C19, and 1A2, respectively (N = 2, <10% variability). ^cN = 3, coefficient of variation < 6%.

The key PKPD parameters for interpreting the LH inhibition data are the unbound plasma and brain levels normalized with respect to the bioactivity, i.e., C_{plasma,u}/K_i and C_{brain,u}/K_i (Table 3).¹ The plasma and brain levels were determined at the T_{max} for the minimum effective dose (MED). As noted before for **2** and **8**,¹ a statistically significant effect was attained at C_{plasma,u}/K_i ≥ 7.6 and C_{brain,u}/K_i > 1 in rat oral LH inhibition studies. This was also the case here, i.e., for analogues **3**, **12**, and **16–18**, with MED values ranging from 3 mg/kg (**3**) to 30 mg/kg (**12** and **17**). For example, in rats, **3** was 20-fold more efficacious in vivo against the initial POC lead **2** despite being 3-fold right-shifted in K_i. This ameliorated efficacy is reflected in their respective MED-normalized plasma and brain PKPD parameters (Table 3, the last two columns). Otherwise stated, the >1-log LLE

superiority of **3** vs **2** underscores the greater unbound exposure levels and consequently the greater in vivo efficacy of **3**. Likewise, the monkey LH data (Figure 2) mirrored these trends with **3** 4-fold more efficacious (MED levels) although nearly equipotent to **2** in monkey K_i values (Table 3) in keeping with the significantly better MED-normalized plasma PKPD parameter for **3** vs **2**.

In summary, **3** proved a superior lead candidate based on bioactivity, LLE, LE, and Fsp³ (Table 1) criteria. Apart from its excellent hERG and CYP safety profile, **3** was highly efficacious in LH inhibition, showed >2.5-log selectivity against NK₁R and NK₂R subtypes, proved >300-fold selective against related HPG axis receptors¹ (KOR, GnRH, GnIH-R, GPR54), and was highly selective in the broad CEREP off-target screen (<25%

Table 2. Permeability, Plasma and Brain Fraction Unbound, Brain Exposure, and PK Data^a

Cpd	Caco-2 P_{app} (nm/sec)			species	plasma f_u	brain f_u	$C_{plasma,u}$ (nM)	$C_{brain,u}$ (nM)	(B/P) _u	iv Cl_T (min/mL/kg)	iv V_{ss} (L/kg)	iv $T_{1/2}$ (min)	%F
	AB	BA	ER										
2 ^b	339	224	0.7	rat	0.055	0.028	54.4	7.79	0.14	7.4	1.4	126	119
2 ^c	—	—	—	monkey	0.043	—	17.9	—	—	16.5	1.52	210	12
3 ^b	487	465	1.0	rat	0.639	0.525	1507	343	0.23	1.5	0.60	279	62.5
3 ^c	—	—	—	monkey	0.532	—	5040	—	—	3.17	1.15	324	107
8 ^d	360	221	0.6	rat	0.065	0.031	58.6	39.3	0.67	7.3	2.8	267	—
12 ^d	477	528	1.1	rat	0.674	0.436	1767	212	0.12	1.94	0.65	239	126
15 ^d	467	345	0.7	rat	0.408	—	—	—	—	2.2	0.91	294	73.6
16 ^d	419	368	0.9	rat	0.291	0.109	348.0	85.4	0.25	1.07	2.25	1479	98.2
17 ^d	437	519	1.2	rat	0.592	0.604	406.7	68.6	0.17	13.7	0.68	35	55
18 ^d	91	345	3.8	rat	0.662	0.995	897.4	45.6	0.05	5.07	1.59	215	46.6

^aPK doses: iv, 1 mg/kg (rat), 10 mg/kg (monkey); oral, 3 mg/kg (rat), 5 mg/kg (monkey). Brain exposure dose: 1 mg/kg. Mean values for $N = 3-4$ rats, or 4 monkeys, per group. All rat data at 60 min: $(B/P)_u = C_{brain,u}/C_{plasma,u}$ with $C_{brain,u} = C_{brain,total} \times bf_u$ and $C_{plasma,u} = C_{plasma,total} \times f_u$. Monkey $C_{plasma,u}$ data at 90 min (oral). ^bPK formulation: HP β CD. ^cPK formulation: iv HP β CD; oral 0.5% MC/water. ^dPK formulation: 1% DMSO, HP β CD in 0.9% NaCl.

Table 3. PKPD Analysis of the Oral LH Inhibition Studies^a

Cpd	species	K_i (nM)	LLE	MED (mg/kg)	T_{max} (min)	$C_{plasma,u}/K_i$	$C_{brain,u}/K_i$	$(C_{plasma,u}/K_i)/MED$	$(C_{brain,u}/K_i)/MED$
2	rat	76	4.0	60	150	16.4	2.32	0.273	0.039
2	monkey	20	4.6	20	60	13.3	—	0.665	—
3	rat	219	5.2	3	150	22.0	5.03	7.33	1.68
3	monkey	25	6.1	5	90	192	—	38.4	—
8	rat	22	4.6	10	150	15.0	12.4	1.5	1.24
12	rat	2033	4.5	30	150	22.5	2.77	0.75	0.09
16	rat	85	4.7	10	150	23.8	5.87	2.38	0.59
17	rat	573	4.9	30	45	47.3	7.71	1.58	0.26
18	rat	244	5.6	10	45	38.9	1.82	3.89	0.18

^aPlasma concentrations coincident with LH measurements. MED determined by a significant decrease ($p < 0.05$) in LH vs baseline with a lower nonsignificant dose established in all cases.

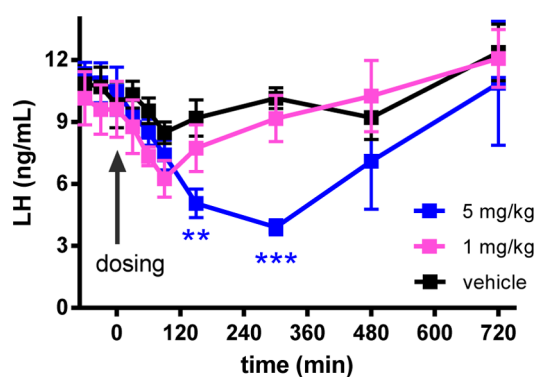


Figure 2. Oral LH inhibition with 3 (0.5% MC/water) in castrated cynomolgus monkey (2-way ANOVA and Dunnet's comparison to the vehicle; *** $p < 0.001$, ** $p < 0.01$).

inhib at 10 μ M). Finally, 3 showed no effect either in Langendorff cardiac safety in rabbits (up to 30 μ M) or in AMES genotoxicity test (up to 100 μ M). Compound 3 (ESN364) is currently in phase 2 clinical trials for the treatment of PCOS and UF.

■ ASSOCIATED CONTENT

Supporting Information

Experimental details for the synthesis and characterization of compounds, X-ray structure of 3 (accession code: CCDC 1052911), and pharmacology and profiling assays. The

Supporting Information is available free of charge on the ACS Publications website at DOI: 10.1021/acsmchemlett.5b00117.

■ AUTHOR INFORMATION

Corresponding Author

*E-mail: hhoveyda@euroscreen.com. Tel: +32-71.348.502.

Funding

This work was supported by the Ministry of Sustainable Development and Public Works, Walloon Region, Belgium.

Notes

The authors declare no competing financial interest.

Biography

Hamid Hoveyda obtained his Ph.D. from the University of British Columbia (Vancouver, Canada) followed by postdoctoral stints at Harvard University (NSERC fellow) and University of Alberta (Edmonton, Canada). He began his industrial career at the Affymax Research Institute (CA, USA) working on the applications of diversity-oriented synthesis in drug discovery. Later, at Tranzyme Pharma (Canada), he led the discovery of two ghrelin agonists that advanced into clinical development for the treatment of GI disorders. Since 2007, he has led medicinal chemistry efforts on various GPCR targets at Euroscreen (Belgium). His scientific contributions have been captured in over fifty publications and patents.

ACKNOWLEDGMENTS

We thank Prof. Tony Plant and Dr. Suresh Ramaswamy (University of Pittsburgh) for the monkey LH assays.

ABBREVIATIONS

ARC, arcuate nucleus; AST, aspartate transaminase; ALT, alanine aminotransferase; bf_w , brain fraction unbound; $(B/P)_w$, unbound brain-to-plasma; CYP, cytochrome P-450; FSH, follicle-stimulating hormone; Fsp^3 , fraction sp^3 carbon content; f_w , plasma fraction unbound; GnRH, gonadotropin-releasing-hormone; HBA, hydrogen-bond acceptor; hERG, human ether-à-go-go related gene; $HP\beta CD$, 9% hydroxypropyl- β -cyclodextrin; HPG, hypothalamic-pituitary-gonadal; KNDy, kisspeptin-neurokinin B-dynorphin A neuron; LH, luteinizing hormone; LE, ligand efficiency; LLE, ligand lipophilicity efficiency; MC, methyl cellulose; MED, minimum effective dose; NKB, neurokinin B; NK_3R , neurokinin-3 receptor; P_{gp} , P-glycoprotein; PKPD, pharmacokinetic-pharmacodynamic; POC, proof-of-concept; $T_{1/2}$, elimination half-life; V_{ss} , steady-state volume of distribution

REFERENCES

- (1) Hoveyda, H. R.; Fraser, G. L.; Roy, M.-O.; Dutheil, G.; Batt, F.; El Bousmaqui, K. J.; Lenoir, F.; Lapin, A.; Noël, S.; Blanc, S. Discovery and optimization of novel antagonists to the human neurokinin-3 receptor for the treatment of sex-hormone disorders (Part I). *J. Med. Chem.* **2015**, *58*, 3060–3082 (Cpds **1**, **2**, and **8** were reported in ref 1 as **3**, **31**, and **39**, respectively.).
- (2) Dawson, L. A.; Porter, R. A. Progress in the development of neurokinin 3 modulators for the treatment of schizophrenia: molecule development and clinical progress. *Future Med. Chem.* **2013**, *5*, 1525–1546 and references therein.
- (3) For a recent review, see: Skorupskaite, K.; George, J. T.; Anderson, R. A. The kisspeptin-GnRH pathway in human reproductive health and disease. *Hum. Reprod. Update* **2014**, *0*, 1–16.
- (4) Marshall, J. C.; Griffin, M. L. The role of changing pulse frequency in the regulation of ovulation. *Hum. Reprod.* **1993**, *8*, 57–61.
- (5) Francou, B.; Bouligand, J.; Voican, A.; Amazit, L.; Trabado, S.; Fagart, J.; Meduri, G.; Brailly-Tabard, S.; Chanson, P.; Lecomte, P.; Guiochon-Mantel, A.; Young, J. Normosomic congenital hypogonadotropic hypogonadism due to *TAC3/TACR3* mutations: characterization of neuroendocrine phenotypes and novel mutations. *PLoS One* **2011**, *6*, e25614.
- (6) Fraser, G. L.; Hoveyda, H. R.; Clarke, I. J.; Ramaswamy, S.; Plant, T. M.; Rose, C.; Millar, R. P. The NK_3 receptor antagonist ESN364 interrupts pulsatile LH secretion and moderates levels of ovarian hormones throughout the menstrual cycle. *Endocrinology*, submitted for publication.
- (7) Riggs, M. M.; Bennets, M.; van der Graaf, P. H.; Martin, S. W. Integrated pharmacometrics and systems pharmacology model-based analysis to guide GnRH modulator development for management of endometriosis. *CPT: Pharmacometrics Syst. Pharmacol.* **2012**, *1*, e11.
- (8) Millar, R. P.; Newton, C. L. Current and future applications of GnRH, kisspeptin and neurokinin B analogues. *Nat. Rev. Endocrinol.* **2013**, *9*, 451–466 and references therein.
- (9) Hopkins, A. L.; Keserü, G. M.; Lesson, P. D.; Rees, D. C.; Reynolds, C. H. The role of ligand efficiency metrics in drug discovery. *Nat. Rev. Drug Discovery* **2014**, *13*, 105–121 and references therein.
- (10) Leeson, P. D.; Empfield, J. R. Reducing the risk of drug attrition associated with physicochemical properties. *Annu. Rep. Med. Chem.* **2010**, *45*, 381–391 and references therein.
- (11) $LE = (1.37/HAC) \times pK_a$. HAC = number of non-hydrogen atoms (ref 9).
- (12) Lovering, F.; Bikker, J.; Humblet, C. Escape from flatland: increasing saturation as an approach to improving clinical success. *J. Med. Chem.* **2009**, *52*, 6752–6756.
- (13) Kalgutkar, A. S.; Driscoll, J.; Zhao, S. X.; Walker, G. S.; Shepard, R. M.; Soglia, J. R.; Atherton, J.; Yu, L.; Mutlib, A. E.; Munchhof, M. J.; Reiter, L. A.; Jones, C. S.; Doty, J. L.; Trevena, K. A.; Shaffer, C. L.; Ripp, S. L. A rational chemical intervention strategy to circumvent bioactivation liabilities associated with a nonpeptidyl thrombopoietin receptor agonist containing a 2-amino-4-arylthiazole motif. *Chem. Res. Toxicol.* **2007**, *20*, 1954–1965.
- (14) Gramec, D.; Mašič, L. P.; Dolenc, M. S. Bioactivation potential of thiophene-containing drugs. *Chem. Res. Toxicol.* **2014**, *27*, 1344–1358 and references therein.
- (15) Trainor, G. L. The importance of plasma protein binding in drug discovery. *Expert Opin. Drug Discovery* **2007**, *2*, 51–64 and references therein.
- (16) Morita, S.; Miyata, S. Accessibility of low-molecular-mass molecules to the median eminence and arcuate hypothalamic nucleus of adult mouse. *Cell Biochem. Funct.* **2013**, *3*, 668–677.
- (17) Kratochwil, N. A.; Huber, W.; Muller, F.; Kansy, M.; Gerber, P. R. Predicting plasma protein binding of drugs: a new approach. *Biochem. Pharmacol.* **2002**, *64*, 1355–1374.
- (18) Kerns, E. H.; Di, L. *Drug-like Properties: Concepts, Structure Design and Methods: from ADME to Toxicity Optimization*; Elsevier: Burlington, MA, 2008; pp 112–116.
- (19) For example, see: Godbole, A. M.; Ramalingam, S.; Ramamurthy, V. P.; Khandelwal, A.; Bruno, R. D.; Upreti, V. V.; Gediya, L. K.; Purushottamachar, P.; Mbatia, H. W.; Addya, S.; Ambulos, N.; Njar, V. C. O. VN/14–1 induces ER stress and autophagy in HP-LTLC human breast cancer cells and has excellent oral pharmacokinetic profile in female Sprague-Dawley rats. *Eur. J. Pharmacol.* **2014**, *734*, 98–104 and references therein.